Saudi Journal of Biological Sciences 29 (2022) 2772–2781

Contents lists available at ScienceDirect

Saudi Journal of Biological Sciences

journal homepage: www.sciencedirect.com

Original article

Comparative study of antifungal activity of two preparations of green silver nanoparticles from *Portulaca oleracea* extract

Fatimah Al-Otibi *, Shahad A. Alfuzan, Raedah I. Alharbi, Abdulaziz A. Al-Askar, Rana M. AL-Otaibi, Hajar F. Al Subaie, Nadine M.S. Moubayed

Department of Botany and Microbiology, College of Science, King Saud University, P.O. Box 22452, Riyadh 11495, Saudi Arabia

ARTICLE INFO

Article history:
Received 6 May 2021
Revised 7 August 2021
Accepted 28 December 2021
Available online 3 January 2022

Keywords:
Antifungal activity
Aqueous extract
Green silver nanoparticles
Gamma irradiation
Portulaca oleracea
Plant pathogenic fungi

ABSTRACT

The green silver nanoparticles (green AgNPs) exhibit an exceptional antimicrobial property against different microbes, including bacteria and fungi. The current study aimed to compare the antifungal activities of both the crude aqueous extract of *Portulaca oleracea* or different preparations of green AgNPs biosynthesized by mixing that aqueous extract with silver nitrate ($AgNO_3$). Two preparations of the green AgNPs were synthesized either by mixing the aqueous extract of *P. oleracea* with silver nitrate ($AgNO_3$) (normal AgNPs) or either irradiation of the AgNPs, previously prepared, under ^{60}Co γ-ray using chitosan (gamma-irradiated AgNPs). Characterization of different AgNPs were tested by Zeta potential analyzer, Ultraviolet (UV) Visible Spectroscopy, and Fourier-Transform Infrared (FTIR) spectrometry. Three different plant pathogenic fungi were tested, *Curvularia spicifera*, *Macrophomina phaseolina*, and *Bipolaris* sp. The antifungal activities were evaluated by Transmission Electron Microscope (TEM) for either the crude aqueous extract of *P. oleracea* at three doses (25%, 50%, and 100%) or the newly biosynthesized AgNPs, normal or gamma-irradiated. With a few exceptions, the comparative analysis revealed that the irradiated green AgNPs at all three concentrations showed a relatively stronger antifungal effect than the normal AgNPs against all the three selected fungal strains. UV–visible spectroscopy of both preparations showed surface plasmon resonance at 421 nm. TEM results showed that both AgNPs were aggregated and characterized by a unique spherical shape, however, the gamma-irradiated AgNPs were smaller than the non-irradiated AgNPs (0.007–0.026 μM vs. 0.009–0.086 μM). TEM photographs of the fungal strains treated with the two AgNPs preparations showed flaccid structures, condensed hyphae, and shrunken surface compared with control cells. The data suggested that the biosynthesized *P. oleracea* AgNPs have antifungal properties against *C. spicifera*, *M. phaseolina*, and *Bipolaris* sp. These AgNPs may be considered a fungicide to protect different plants against phytopathogenic fungi.

1. Introduction

Portulaca oleracea L., which is commonly known as *Purslane*, the duckweed or the little hogweed, a flowering plant and a member of the *Portulacaceae* family (order *Caryophyllales*), comprises 30 genera and about 500 species including some small herbaceous plants and herbs such as *Portulaca pilosa* and *Avonia ustulate* (Zhou et al., 2015). It's a widespread annual succulent edible herb that was a traditional folk medicine that acted as a vermifuge, febrifuge, and antiseptic in the North African, Asian, and European countries, besides, the tropical and subtropical regions (Zhou et al., 2015; Iranshahy et al., 2017).

The chemical analysis of the *P. oleracea* revealed a high content of phytochemicals. Previous studies reported that its extract contains different proteins, soluble carbohydrates, inorganic acids, flavonoids, alkaloids, cardiac glycosides, coumarins, tannins, saponin, and anthraquinone glycosides (Achilonu et al., 2018; Nagarani et al., 2014). The leaves of *P. oleracea* contain a high level of magnesium, omega-3 fatty acids, and α-linolenic acid (Nagarani et al., 2014; Rahimi et al., 2019). Previous studies haven't reported the full medicinal properties of the *P. oleracea*. Despite that, some recent studies showed that its crude extract exhibited antibacterial (Mousavi et al., 2015), antifungal (Du et al., 2017), antiviral (Li

* Corresponding author.
E-mail address: falotibi@ksu.edu.sa (F. Al-Otibi).

Peer review under responsibility of King Saud University.

Production and hosting by Elsevier

https://doi.org/10.1016/j.sjbs.2021.12.056
1319-562X/

et al., 2019), anti-inflammatory (Allahmoradi et al., 2018), antiulcerogenic, antioxidant, and wound-healing properties (Achilonu et al., 2018). Another study showed that the ethanolic extract of *P. oleracea* inhibited the growth of the pathogenic yeast *Candida albicans* (Soliman, et al., 2017).

Macrophomina phaseolina (*M. phaseolina*) is a soil-borne fungal pathogen with heterogeneous host septicity. It causes seedling blight, damping off, and rot (collar, stem, basal stem, and root) in many plant species (Mayék-Pérez et al., 2001). *Bipolaris* sp. is a common phytopathogenic fungi that cause leaf blights and spots, melting outs, root and foot rots, and other diseases in high-value field crops, such as rice, maize, wheat, sorghum, and other host plants (Manamgoda et al., 2014). *Curvularia spicifera* (*C. spicifera*) is another phytopathogen that causes the leaf blights, and rotting of the fruit and stem in date and ornamental palms. It occasionally affects wheat, rice, barley, and other cereals (Qostal et al., 2019).

The green silver nanoparticle is a recent technique that synthesis silver nanoparticles (AgNPs) in combination with plant-derived phytochemicals (AlSalhi et al., 2019). Previous studies reported that the green AgNPs exhibited different antimicrobial activities (Mallmann et al., 2015; Qing et al., 2018). The relative ease of preparation of green AgNPs, the low cost, and eco-friendly applications are the most reported advantages (Ahmed and Mustafa, 2020; Abbasi et al., 2019; Singh et al., 2019).

In the current study, we compared the antifungal activity of either the normal or gamma-irradiated silver nanoparticles (AgNPs) synthesized in combination with the aqueous extract of *P. oleracea*. Different fungal species were used, included *C. spicifera*, *M. phaseolina*, and *Bipolaris* sp. Moreover, the Fourier-transform infrared (FTIR) spectroscopy was applied to identify the phytochemical composition of the synthesized AgNPs. Besides, the transmission electron microscopy (TEM) characterized the ultrastructural damage induced by the two green AgNPs preparations.

2. Materials and methods

2.1. Sample's collection and preparation of the P. oleracea aqueous extract

P. oleracea was collected from a local garden in Buraydah governorate, Al-Qassim Region, Saudi Arabia. The fresh leaves were washed carefully with deionized water, air-dried at room temperature, then sliced into small pieces with sterile scissors. An amount of 2.5 g of the fresh sliced leaves were soaked in deionized water at 10% (w/v). The leaves were boiled by using a hot plate supplied with a magnetic stirrer (Fig. 1). The mixture was then cooled and filtered by Whatman® qualitative filter paper (Sigma-Aldrich, St. Louis, Missouri, USA). The filtrate was clear and colorless with an acidic pH of 4.5. The extract was preserved aseptically in glass bottles at 4 °C for further use.

2.2. Synthesis of the green AgNPs using P. oleracea aqueous extract

The microwave-assisted extraction technique was employed to biosynthesize silver nanoparticles (Joseph and Mathew, 2014; Seku et al., 2018). AgNPs were prepared either normally or by gamma-irradiation at three different concentrations (100%, 50%, and 25%). For example, for the synthesis of the normal AgNPs, we mixed 1 mL of the *P. oleracea* aqueous extract with 1 mM of silver nitrate ($AgNO_3$) solution (100%), as described previously (Mohammed et al., 2018). The mixture was then boiled with continuous stirring for a few minutes until the colorless aqueous extract turned yellowish-brown because of the extracellular synthesis of nanoparticles (Guilger-Casagrande and de Lima, 2019). The synthesis of the gamma-irradiated AgNPs was by irradiating the normal AgNPs under ^{60}Co γ-ray using chitosan (Nhien et al., 2018). The radiating of the normal AgNPs solution was optimized at a fixed dose rate of 40.9 Gy/min and at different time points. Then, stabilization of the got AgNPs took place in a dilute irradiation-degrade chitosan solution (Phu et al., 2014).

2.3. Fungal specimens

The fungal strains were identified and obtained from the Department of Botany and Microbiology, College of Sciences, King Saud University, Riyadh, Saudi Arabia. The fungi included *C. spicifera* (NCBI Taxonomy ID:145392, accession number: MT497471.1), *M. phaseolina* (NCBI Taxonomy ID: 35725, accession number: MN128590), and *Bipolaris* sp. (NCBI Taxonomy ID: 339742, accession number: MN978926). The fungal isolates were cultured and maintained on potato dextrose agar. The strains were stored at 4 °C or sub-cultured once a month for further uses.

2.4. Antifungal screening

The antifungal activity of the synthesized green AgNPs of the crude aqueous extract of *P. oleracea* was investigated using the poisoned food technique (Gakuubi et al., 2017). Briefly, one mL of different AgNPs at the three different doses (100%, 50%, and 25%) was, aseptically, poured into sterile Petri dishes. Then, the volume of 19 mL of molten potato dextrose agar was poured and solidified. At nine days old, either *C. spicifera*, *M. phaseolina*, or *Bipolaris* sp. cultures were seeded, separately, into the central area of the Petri dishes for more seven days at 25 ± 2 °C. An untreated control petri dish was used for comparison. The percentage of the inhibition in mycelial growth (IMG) was calculated as follows:

$$\%\ \mathrm{IMG} = \frac{\mathrm{dC} - \mathrm{dT}}{\mathrm{dC}} X100$$

where dC and dT are the mean diameters of the mycelial growth in the control and treated plates, respectively (Costa et al., 2015).

2.5. Characterization of biosynthesized green AgNPs

The characteristics of the synthesized green AgNPs were determined by the UV–visible spectroscopy, Libra S22 (Biochrom PVT, Cambridge, UK) at a resolution of 200–800 nm. The size and morphological characteristics of AgNPs were determined by TEM, JEM-1011 (JEOL, Peabody, MA, USA). FTIR spectroscopy by Nicolet 6700 FT-IR (Thermo Fisher Scientific, MS, USA) which is supplied with a beam splitter and a detector, where the configuration of the functional constituents in AgNPs preparations were analyzed by OMNIC software (Alotibi and Rizwana, 2019). Finally, the Zeta potential analyzer, Zeta sizer Nanoseries HT (Malvern Panalytical, Malvern, UK) was used to detect the surface charge of AgNPs in the solution.

2.6. Statistical analysis

As all experiments were carried out in triplicates, the means and standard deviations were calculated using GraphPad Prism 6. Significant differences between results were evaluated by IBM SPSS Statistics 22.0 by the analysis of variance tool, *One-way ANOVA*. The significance levels were set at $P < 0.05$.

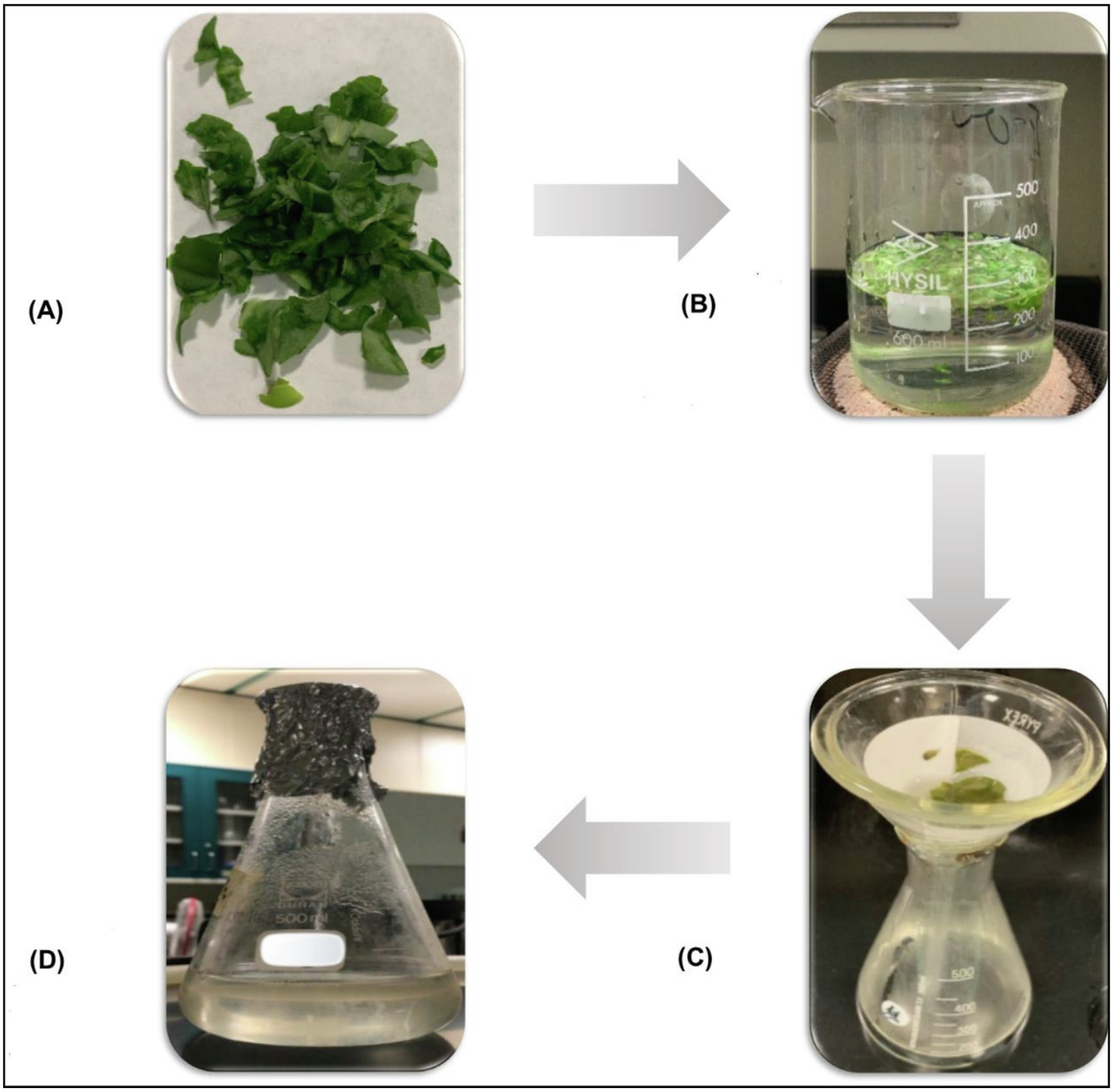

Fig. 1. Schematic representation of the aqueous extract preparation from the *P. oleracea* leaves. A) Leaves slicing, B) Boiling in deionized water, C) extract filtration, D) Ready-to-use aqueous extract of *P. oleracea* leaves.

3. Results

3.1. The biogenic properties of AgNPs of P. oleracea aqueous extract:

The morphological, chemical and physical properties of the synthesized AgNPs of *P. oleracea* had been tested. Characterization of normal and gamma-irradiated AgNPs using UV–visible spectroscopy showed a strong peak at approximately 421 nm, which could be because of the surface plasmon resonance (SPR) band of AgNPs. There were characteristic differences observed in the absorption spectra of both AgNPs (Fig. 2).

Results from TEM revealed the morphological characteristics of the synthesized AgNPs. Both types of AgNPs were aggregated and characterized by a unique spherical shape. The image analysis estimated the size of the gamma-irradiated AgNPs to range from 0.007 to 0.026 μM (Fig. 3**A**) where the size of the normal AgNPs ranges from 0.009 to 0.086 μM (Fig. 3**B**).

FTIR spectroscopic analysis of the synthesized AgNPs revealed almost similar estimated composition (Fig. 4). In the normal AgNPs, FTIR showed medium absorption peaks at 3267, 2181, and 1635 cm^{-1} which are corresponding, respectively, to alcohol, alkyne, and alkylamines, besides four weak sharp peaks at 2160, 2150, 1987, and 1959 cm^{-1} which correspond to azide, thiocyanate, ketones, and aromatic compounds, respectively (Fig. 4**A; **Table 1). Similarly, FTIR analysis of the gamma-irradiated AgNPs showed medium absorption peaks at 3260, 2207, 2173, 2042, 2026, and 1634 cm^{-1} which are corresponding to alcohol, alkyne, thiocyanate, and alkylamines, besides four weak sharp peaks at 2159, 2104, 1988, and 1960 cm^{-1} which correspond to azide, alkyne, and aromatic compound, respectively (Fig. 4**B;** Table 1).

The Zeta potential analysis detected the mean diameter size of the normal *P. oleracea* AgNPs to be 117.4 nm with a polydispersity index (PdI) value of 0.167 and an intercept of 0.901 which was represented by one specific peak at 100% intensity and size of 142.9 ± 58.3 nm (Fig. 5**A**). Unlikely, the average particle size of the gamma-irradiated *P. oleracea* extracts AgNPs was smaller at Z-average of 69.09 nm, with a PdI value of 0.243 and an intercept of 0.869 which was represented by two peaks at the sizes of 94 ± 41.3 nm (95%) and 15 ± 3.1 nm (5%) (Fig. 5**B**).

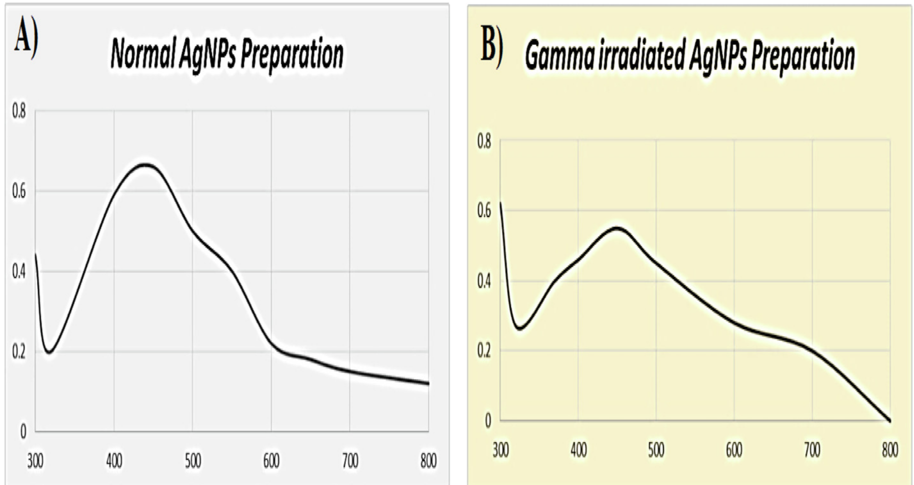

Fig. 2. UV–visible spectra of AgNPs assessed by Libra S22 A) spectra of normal AgNPs, B) spectra of gamma-irradiated AgNPs. UV, ultraviolet.

3.2. Antifungal activity of silver nanoparticles of aqueous extract of P. oleracea

Both normal and irradiated silver nanoparticle preparations of *P. oleracea* extract inhibited the mycelial growth of *C. spicifera*, *M. phaseolina*, and *Bipolaris* sp. Different concentrations didn't show any markable differences in the percentage of inhibition of the mycelial growth of the three fungal strains. Comparative analysis revealed that, with a few exceptions, the irradiated green AgNPs at all three concentrations showed a relatively stronger antifungal effect than the normal AgNPs against all the three selected fungal strains (Table 2). The control plates (untreated) showed confluent normal mycelial growth for all fungi (Fig. 6).

TEM microphotographs revealed the morphological changes induced by different AgNPs treatments against the strains of *C. spicifera*, *M. phaseolina*, and *Bipolaris* sp. (Fig. 7). The untreated strains showed the mycelia with intact to a normal tubular structure (left panel). The fungi treated with the normal AgNPs showed distended and flaccid structures with condensed hyphal branches and rough/shrunken surfaces (middle panel). Similarly, distorted structures were observed for all the three fungal strains treated with the gamma-irradiated green AgNPs (right panel).

4. Discussion

Deserts of the Arabian Peninsula countries are rich sources of many wild plants and herbs of medical importance (Chaurasia and Gharia, 2017). The antifungal activity of *P. oleracea* different extracts was well-studied against different bacterial and fungal species (Mousavi et al., 2015; Du et al., 2017). Multiple studies suggested that different preparations of plant extracts using ethanol, chloroform, or other solvents could affect the pharmacological and morphological properties of the growth of some species such as *Trichophyton* sp. (Oh et al., 2000) and *Candida ablicans* (Soliman et al., 2017) more than the aqueous extract (Chaurasia and Gharia, 2017). However, recent studies showed that aqueous extract of *P. oleracea* leaves which had a greater content of phenolic and flavonoids compounds 210.4 ± 1.15 and 36.7 ± 0.79 mg/mL)

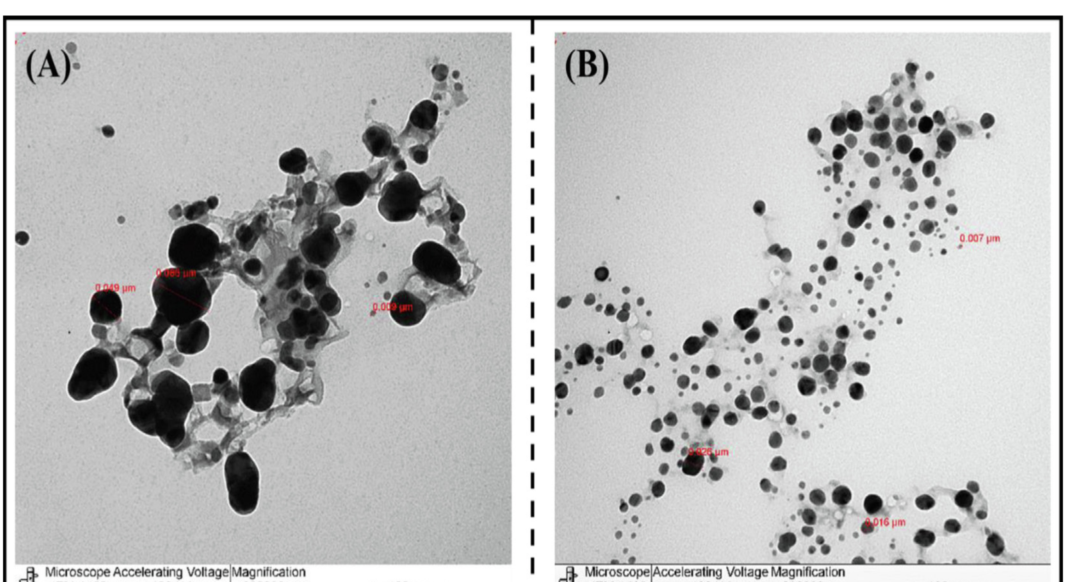

Fig. 3. TEM microphotographs of the synthesized green silver nanoparticles of *P. oleracea* extract by JEM-1400, the diameter of the particles was calculated in μM with a magnification of 200,000×. (A) Normal AgNPs (without irradiation) and (B) Gamma-irradiated AgNPs. TEM; Transmission Electron Microscopy.

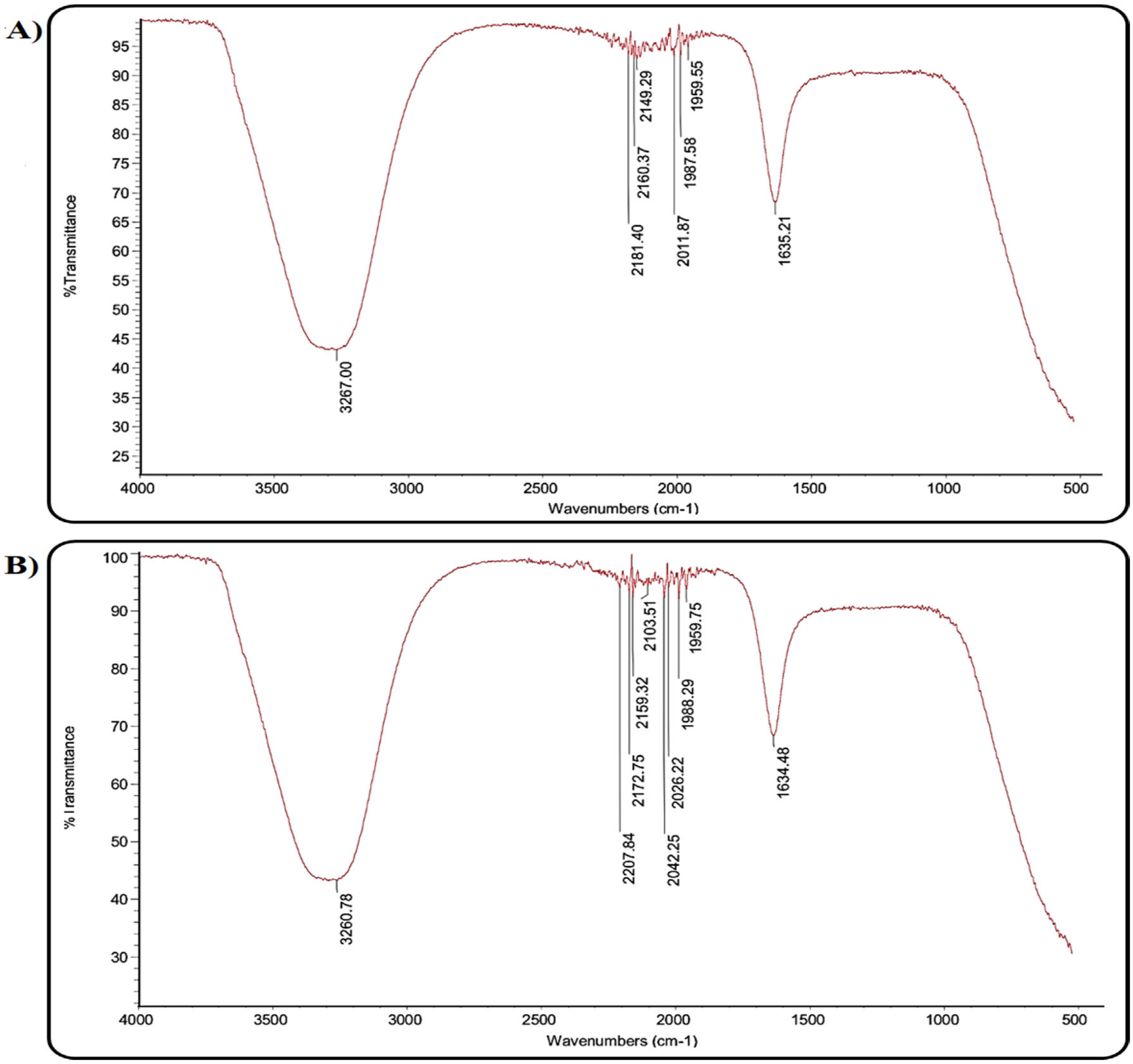

Fig. 4. Fourier-transform infrared (FTIR) spectrum of synthesized AgNPs of *P. oleracea* extract. A) Normal AgNPs, B) Gamma-irradiated AgNPs.

Table 1
The functional group analysis by FTIR.

Tested material	Absorption (cm^{-1})	Appearance	Group	Compound Class
Normal AgNPs	3267	Medium, broad	O—H stretching	Alcohol, intramolecular bonded
	2181	Medium	C≡C stretching	Alkyne, disubstituted
	2160	Weak	N═N═N stretching, S—C≡N stretching	Azide or Thiocyanate
	2150	Weak	C═C═O stretching	ketene
	1987, 1960	Weak	C—H bending	Aromatic compound, overtone
	1635	Medium, sharp	C═C stretching, N—H bending	Alkene or Amine
	2011	Medium		None
Gamma-irradiated AgNPs	3261	Medium, broad	O—H stretching	Alcohol, intramolecular bonded
	2207	Medium	C≡C stretching	Alkyne, disubstituted
	2173	Medium	S—C≡N stretching	Thiocyanate
	2159	Weak	N═N═N stretching	Azide
	2104	Weak	C≡C stretching	Alkyne, monosubstituted
	2042, 2026	Medium	N=C=S stretching	Isothiocyanate
	1988, 1960	Weak	C—H bending	Aromatic compound, overtone
	1634	Medium, sharp	C═C stretching, N—H bending	Alkene or Amine

could inhibit the growth of different fungal and bacterial strains belong to *Aspergillus* sp. (El-Desouky, 2021), *Helicobacter pylori*, *Staphylococcus epidermidis*, *Staphylococcus aureus*, *Streptococcus mutan*, and *Escherichia coli* (Cho et al., 2008; Sun et al., 2015). In the study conducted by Sun et al., (2015), the aqueous extract of *P. oleracea* leaves (0.25 g/ml) was more effective against *Escherichia*

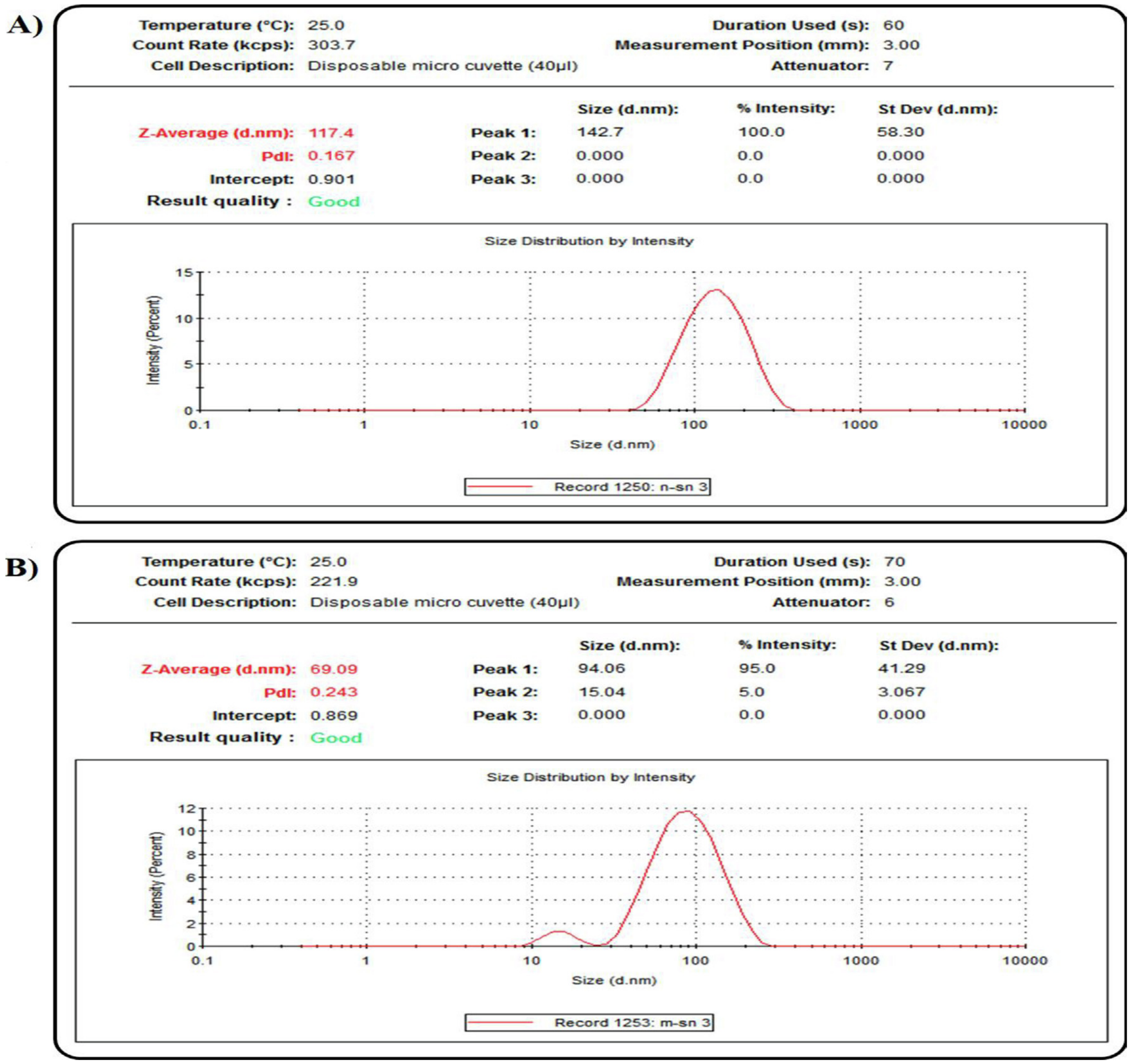

Fig. 5. The intensity percentage describing the particle size distribution of biosynthesized AgNPs of *P. oleracea* extract. A) Normal AgNPs, B) Gamma-irradiated AgNPs. UV, ultraviolet; PdI, polydispersity index.

coli as it showed larger inhibition zone (19.2 ± 0.19 mm) than the ethanolic extract (19.2 ± 0.19 mm).

In the present study, the antifungal activity of silver nanoparticles of the aqueous extract of *P. oleracea* was investigated. The synthesis of AgNPs followed the eco-friendly green route method to create two different preparations of nanoparticles, including the normal and gamma-irradiated AgNPs, to screen their inhibitory effect on the mycelial growth of the selected fungal strains (*C. spicifera*, *M. phaseolina*, and *Bipolaris* sp.). The results of the UV-spectrum analysis showed that the biosynthesized AgNPs presented an excitonic absorption edge at 400–500 nm which confirmed their formation. Regarding that, a previous study showed that synthesized AgNPs had a unique band of SPR at 400–500 nm compared to $AgNO_3$ such as the AgNPs of *Cornus officinalis* extract (Wang et al., 2020) and *Coptidis rhizome* (Sharma et al., 2018). Besides, the analysis of TEM images confirmed the morphological differences in the sizes of both AgNPs where the gamma-irradiated AgNPs were smaller than the normal AgNPs.

Table 2
Antifungal activity of Normal and Irradiated AgNPs of *P. oleracea* extract.

Fungal species	*Curvularia spicifera*		*Macrophomina phaseolina*		*Bipolaris* sp.	
	Growth* (mm)	% IMG	Growth* (mm)	% IMG	Growth* (mm)	% IMG
Control	88.0 ± 0.0	0.00	88.0 ± 0.0	0.00	88.0 ± 0.0	0.00
Normal AgNPs	16.5 ± 5.0	81.25	15.5 ± 4.5	82.39	25.8 ± 9.8	70.68
	12.8 ± 0.3	85.45	16.5 ± 1.0	81.25	26.3 ± 1.8	70.11
	16.0 ± 0.5	81.82	14.0 ± 0.0	84.09	20.3 ± 1.3	76.93
Gamma-irradiated AgNPs	17.8 ± 1.3	79.77	14.3 ± 2.3	83.75	19.0 ± 1.5	78.41
	9.5 ± 2.0	89.20	9.8 ± 0.8	88.86	17.5 ± 6.0	80.11
	17.0 ± 3.5	80.68	13.0 ± 0.5	85.23	15.0 ± 4.0	82.95

*Means ± SD of triplicates.

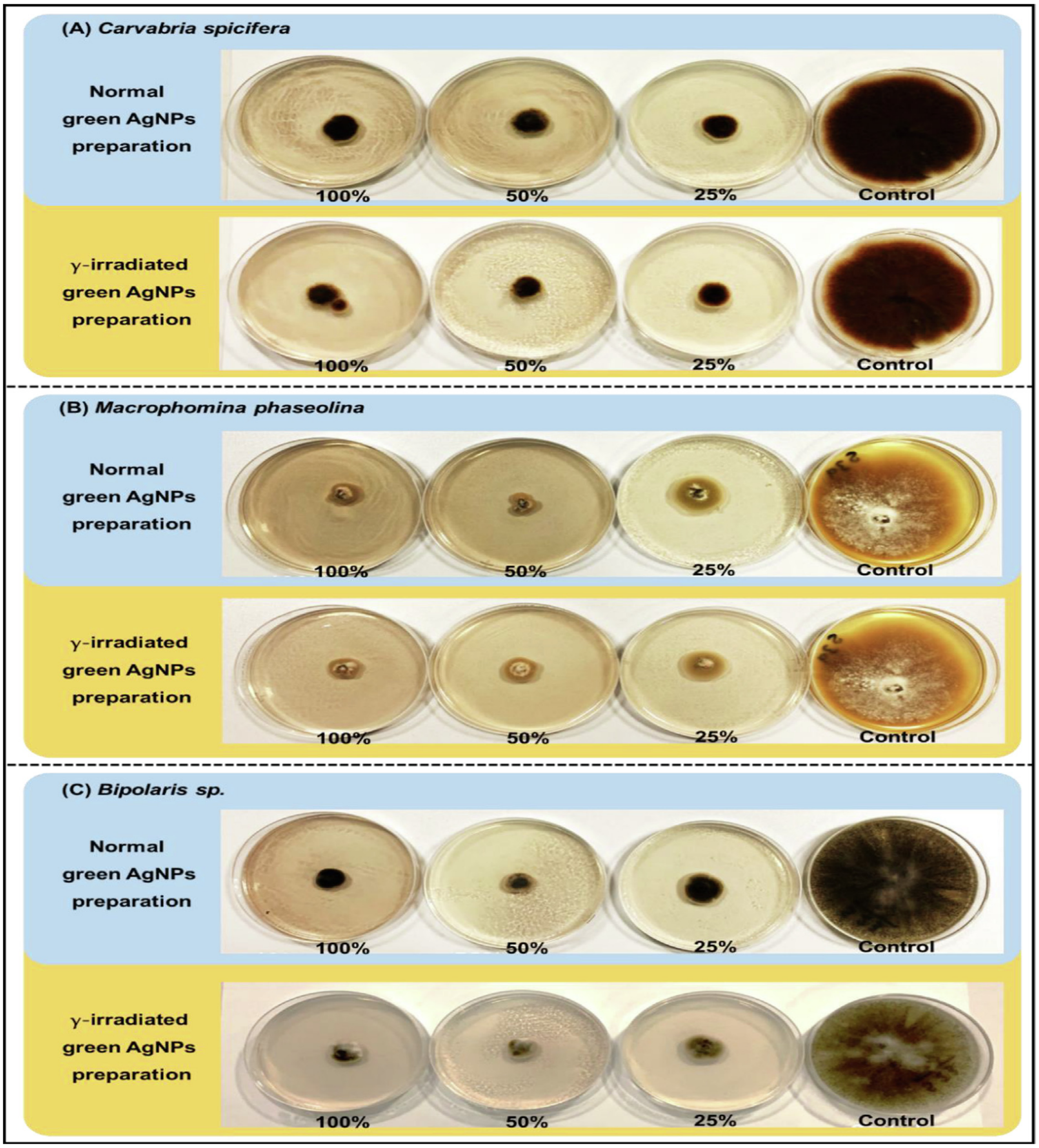

Fig. 6. *In vitro* antifungal activity of three different doses of either normal or gamma-irradiated AgNPs by the poisoned food technique, against. **(A)** *Carvabaria spicifera*, **(B)** *Macrophomina phaseolina* and **(C)** *Bipolaris* sp.

In agreement with these findings, a previous study used TEM and dynamic light scattering (DLS) experiments to screen the characteristics of *Bombyx mori* silk AgNPs irradiated with gamma and showed that it was smaller in size despite it induced more reduction in the mycelial growth (Madhukumar et al., 2017). The phytochemical screening, by FTIR spectroscopy, revealed a remarkable differentiation in the bioactive compound's composition (aliphatic and aromatic) in both AgNPs preparations which might be considered key factors to explain the mechanism of the antifungal activities. Similar findings were reported in the study conducted by Afify et al. (2017), where the FTIR analysis of gamma-irradiated AgNPs showed absorption peaks at 3460, 2850–2900, 1650, 1430, and 1370 cm^{-1} which are assigned to —OH, —CH, C═O, C≡C and C═O stretching vibrations, respectively, which suggested their integrations in the AgNPs synthesis which increase the interaction with other compounds through bonding with the O and N atoms (Afify et al., 2017).

Multiple studies had reported the effectiveness of green AgNPs biosynthesized by plants that suggested them as promising alternatives or natural fungicides to shield plants against different phytopathogenic fungi and overcome the toxic effect imposed by chemical pesticides (Kim et al., 2012). Studies showed that exposure to green AgNPs caused serious cellular deformation by interacting with unsaturated fatty acids which increases the permeability of the cell membranes resulted in the loss of water, salts, proteins, and some intracellular components which affect the vitality and survival of the fungal cells (Durán et al., 2016; Zhang et al., 2018). In the present study, treatments with both preparations of green AgNPs, synthesized by different concentrations of aqueous extract of *P. oleracea*, showed a strong reduction in the mycelial growth of the selected pathogenic fungi. The comparative analysis showed that gamma-irradiated AgNPs exhibited relatively better antifungal activity than the normal green AgNPs. As mentioned before, these variations are thought to be due to the differences in concentrations of the bioactive compounds (aliphatic and aromatic compounds) in both AgNPs preparations (Afify et al., 2017). Other factors such as the method of extraction, pH, solubility, volatility, growth medium composition, and the natural

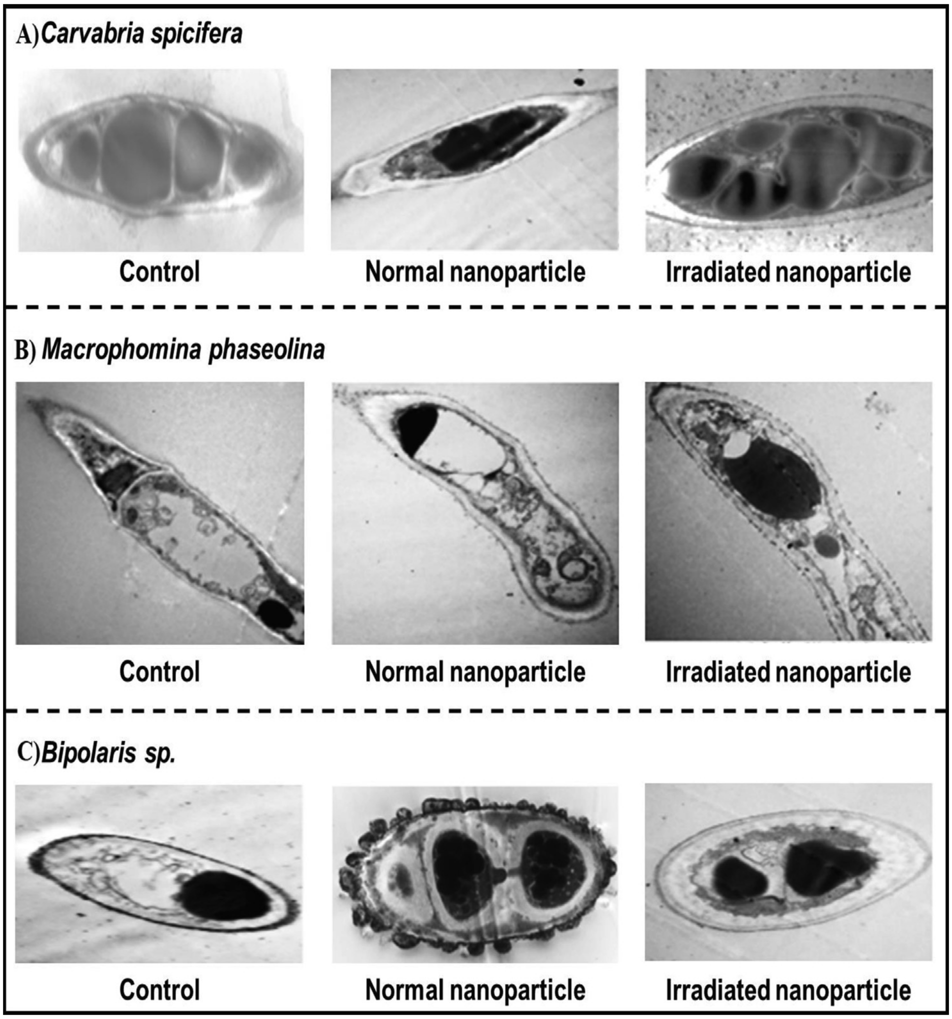

Fig. 7. TEM microphotographs showing the antifungal activity of the synthesized AgNPs of *P. oleracea* extract by JEM-1400 with a magnification of 200,000×. The left panel shows the untreated strains with normal mycelia and tubular structure, the middle panel shows the effect of normal AgNPs treatment and the effect on the hyphal and surface structures, while the right panel shows the gamma-irradiated green AgNPs. A) *Carvabaria spicifera*, **B)** *Macrophomina phaseolina*, and **C)** *Bipolaris* sp. TEM; Transmission Electron Microscopy.

characteristics of the tested species might contribute to the variation in the antifungal activities (Martínez-Martínez et al., 2012; Mohammed et al., 2018). In agreement with our findings, similar studies showed the antifungal activity of colloidal gamma-irradiated AgNPs against *Corticium salmonicolor* (Phu et al., 2010), *Colletotrichum* sp. (Lamsal et al., 2011), *Macrophomina phaseolina*, *A. alternata*, *F. oxysporum*, *Trichoderma harzianum.* and *Geotrichum candidum* induced by treatment with AgNPs synthesized from the *Amaranthus retroflexus* leaf extract (Bahrami-Teimoori et al., 2017).

TEM microphotographs of the fungal species treated with both AgNPs showed different morphological changes in the fungal mycelium compared to untreated controls that endorse their antifungal activity, particularly the gamma-irradiated AgNPs. Gamma-irradiated AgNPs were relatively stronger than normal AgNPs as it caused a greater mycelial reduction in the growth *M. phaseolina* compared with *C. spicifera and Bipolaris* sp. A previous study showed that AgNPs prepared at the 1:10 to the aqueous extract of *P. oleracea* showed 12 mm and 19 mm zone of inhibition against the fungal species of *Candida albicans* and *Saccharomyces cerevisiae*, respectively (Jannathul Firdhouse and Lalitha, 2015). The data suggested that AgNPs of *P. oleracea*, particularly the gamma-irradiated, possess a strong antifungal property and has the potential to be used as a promising antifungal agent against plants against phytopathogenic fungi.

5. Conclusion

The results confirm to the antifungal activity of the aqueous extract of *P. oleracea* leaves and the AgNPs prepared from it against different strains including, *C. spicifera*, *M. phaseolina*, and *Bipolaris* sp. The results revealed that gamma-irradiated AgNPs of *P. oleracea* extract might be more active and possess a relatively greater antifungal activity than the normal AgNPs against the selected phytopathogenic fungi. Further studies are required to understand the molecular mechanism by which green AgNPs of *P. oleracea* extract inhibits the mycelial growth of different fungi, besides, the medicinal properties of the *P. oleracea* which have not been fully explored.

Author’s contribution

The conception and study design were performed by F.A. and S. A.A. R.I.A. and N.M.S.M. were responsible for the literature search. Both of R.M.A. and H.F.A. collected the samples, performed the methodology. The experimental design, data acquisition and analysis, statistical analysis, editing and reviewing of the intellectual contents were carried out by F.A. R.I.A. and A.A.A. prepared the manuscript. F. A. reviewed and edited the manuscript, besides acting as a guarantor and corresponding author. All authors have read and agreed to the published version of the manuscript.

Funding

This research project was supported by a grant from the Researchers Supporting Project number (RSP-2021/114), King Saud University, Riyadh, Saudi Arabia.

Declaration of Competing Interest

The authors declare that they have no known competing financial interests or personal relationships that could have appeared to influence the work reported in this paper.

Acknowledgements

The authors would like to extend their sincere appreciation to the Research Supporting Project number: RSP-2021/114, King Saud University, Riyadh, Saudi Arabia.

References

Abbasi, B.H., Nazir, M., Muhammad, W., Hashmi, S.S., Abbasi, R., Rahman, L., Hano, C., 2019. A comparative evaluation of the antiproliferative activity against HepG2 liver carcinoma cells of plant-derived silver nanoparticles from basil extracts with contrasting anthocyanin contents. Biomolecules 9, 320. https://doi.org/10.3390/biom9080320.

Achilonu, M., Shale, K., Arthur, G., Naidoo, K., Mbatha, M., 2018. Phytochemical benefits of agroresidues as alternative nutritive dietary resource for pig and poultry farming. J. Chem. 2018, 1–15. https://doi.org/10.1155/2018/1035071.

Afify, T.A., Saleh, H.H., Ali, Z.I., 2017. Structural and morphological study of gamma-irradiation synthesized silver nanoparticles. Polym. Compos. 38 (12), 2687–2694. https://doi.org/10.1002/pc.23866.

Ahmed, Reem Hassan, Mustafa, Damra Elhaj, 2020. Green synthesis of silver nanoparticles mediated by traditionally used medicinal plants in Sudan. Int. Nano Lett. 10 (1), 1–14. https://doi.org/10.1007/s40089-019-00291-9.

Allahmoradi, E., Taghiloo, S., 2018. VH.Anti-inflammatory effects of the *Portulaca oleracea* hydroalcholic extract on human peripheral blood mononuclear cells. Med. J. Islam. Repub. Iran. 32, 80. https://doi.org/10.14196/mjiri.32.80.

Alotibi, F.A., Rizwana, H., 2019. Chemical composition, FTIR studies, morphological alterations, and antifungal activity of leaf extracts of *Artemisia sieberi* from Saudi Arabia. Int. J. Agric. Biol. 21, 1241–1248. https://doi.org/10.17957/ijab/15.1017.

AlSalhi, Mohamad S., Elangovan, Kannan, Ranjitsingh, Amirtham Jacob A., Murali, P., Devanesan, Sandhanasamy, 2019. Synthesis of silver nanoparticles using plant derived 4-N-methyl benzoic acid and evaluation of antimicrobial, antioxidant and antitumor activity. Saudi J. Biol. Sci. 26 (5), 970–978. https://doi.org/10.1016/j.sjbs.2019.04.001.

Bahrami-Teimoori, Bahram, Nikparast, Yaser, Hojatianfar, Mostafa, Akhlaghi, Mahdi, Ghorbani, Reza, Pourianfar, Hamid Reza, 2017. Characterisation and antifungal activity of silver nanoparticles biologically synthesised by *Amaranthus retroflexus* leaf extract. J. Exp. Nanosci. 12 (1), 129–139. https://doi.org/10.1080/17458080.2017.1279355.

CHAURASIA, ARTI, GHARIA, ANIL, 2017. Antifungal activity of medicinal plant *Boswellia serrata*. J. Ultra Chem. 13 (04), 88–90.

Cho, Y.J., Ju, I.S., Kwon, O.J., Chun, S.S., An, B.J., Kim, J.H., 2008. Biological and antimicrobial activity of Portulaca oleracea. J. Korean Soc. Appl. Biol. Chem. 51, 49–54.

Costa, L., Pinto, J., Bertolucci, S., Costa, J., Alves, P., Niculau, E., 2015. In vitro antifungal activity of *Ocimum selloi* essential oil and methylchavicol against phytopathogenic fungi. Rev. Cienc. Agron. 46, 2. https://doi.org/10.5935/1806-6690.20150023.

Du, Yong-Kai, Liu, Jing, Li, Xiu-Mei, Pan, Fang-Fang, Wen, Zhi-Guo, Zhang, Tong-Cun, Yang, Pei-Long, 2017. Flavonoids extract from Portulaca oleracea L. induce Staphylococcus aureus death by apoptosis-like pathway. Int. J. Food Prop. 20 (sup1), S534–S542. https://doi.org/10.1080/10942912.2017.1300812.

Durán, Nelson, Durán, Marcela, de Jesus, Marcelo Bispo, Seabra, Amedea B., Fávaro, Wagner J., Nakazato, Gerson, 2016. Silver nanoparticles: a new view on mechanistic aspects on antimicrobial activity. Nanomedicine 12 (3), 789–799. https://doi.org/10.1016/j.nano.2015.11.016.

El-Desouky, Tarek A., 2021. Evaluation of effectiveness aqueous extract for some leaves of wild edible plants in Egypt as anti-fungal and anti-toxigenic. Heliyon 7 (2), e06209. https://doi.org/10.1016/j.heliyon.2021.e06209.

Gakuubi, M. M., Maina, A. W., Wagacha, J. M., 2017. Antifungal Activity of Essential Oil of *Eucalyptus camaldulensis* Dehnh. against Selected *Fusarium* spp. Int. J. Microbiol. 2017, 8761610. https://doi.org/10.1155/2017/8761610.

Guilger-Casagrande, M., de Lima, R., 2019. Synthesis of silver nanoparticles mediated by fungi: a review. Front. Bioeng. Biotechnol. 7, 287. https://doi.org/10.3389/fbioe.2019.00287.

Iranshahy, M., Javadi, B., Iranshahi, M., Jahanbakhsh, S.P., Mahyari, S., Hassani, F.V., Karimi, G., 2017. A review of traditional uses, phytochemistry and pharmacology of *Portulaca oleracea* L. J. Ethnopharmacol. 205,158-172. https://doi.org/10.1016/j.jep.2017.05.004.

Jannathul Firdhouse, M., Lalitha, P., 2015. Biocidal potential of biosynthesized silver nanoparticles against fungal threats. J. Nanostruct. Chem. 5 (1), 25–33. https://doi.org/10.1007/s40097-014-0126-x.

Joseph, S., Mathew, B., 2014. Microwave assisted biosynthesis of silver nanoparticles using the rhizome extract of *Alpinia galanga* and evaluation of their catalytic and antimicrobial activities. J. Nanopart. 2014, 1–9. https://doi.org/10.1155/2014/967802.

Kim, Sang Woo, Jung, Jin Hee, Lamsal, Kabir, Kim, Yun Seok, Min, Ji Seon, Lee, Youn Su, 2012. Antifungal Effects of Silver Nanoparticles (AgNPs) against Various Plant Pathogenic Fungi. Mycobiology 40 (1), 53–58.

Lamsal, Kabir, Kim, Sang Woo, Jung, Jin Hee, Kim, Yun Seok, Kim, Kyong Su, Lee, Youn Su, 2011. Application of Silver Nanoparticles for the Control of *Colletotrichum* Species In Vitro and *Pepper Anthracnose* Disease in Field. Mycobiology 39 (3), 194–199.

Li, Yao-Hsuan, Lai, Chun-Yi, Su, Mei-Chi, Cheng, Ju-Chien, Chang, Yuan-Shiun, 2019. Antiviral activity of *Portulaca oleracea* L. against influenza A viruses. J. Ethnopharmacol. 241, 112013. https://doi.org/10.1016/j.jep.2019.112013.

Madhukumar, R., Byrappa, K., Wang, Youjiang, Sangappa, Y., 2017. Effect of gamma irradiation on synthesis and characterization of bio-nanocomposite SF/Ag nanoparticles. Radiat. Eff. Defects Solids 172 (11-12), 915–921. https://doi.org/10.1080/10420150.2017.1418873.

Mallmann, E., Cunha, F., Castro, B., Maciel, A., Menezes, E., Fechine, P., 2015. Antifungal activity of silver nanoparticles obtained by green synthesis. Rev. Inst. Med. Trop. Sao Paulo. 57 (2), 165–167.

Manamgoda, D., Rossman, A., Castlebury, L., Crous, P., Madrid, H., Chukeatirote, E., Hyde, K., 2014. The genus *Bipolaris*. Stud. Mycol. 79, 221–288. https://doi.org/10.1016/j.simyco.2014.10.002.

Martínez-Martínez, M.U., Herrera-Van Oostdam, D., Román-Acosta, S., Magaña-Aquino, M., Baranda-Cándido, L., Abud-Mendoza, C., 2012. Invasive fungal infections in patients with systemic lupus erythematosus. J. Rheumatol. 39 (9), 1814–1818. https://doi.org/10.3899/jrheum.111498.

Mayék-Pérez, Netzahualcóyotl, López-Castañeda, Cándido, González-Chavira, Mario, Garcia-Espinosa, Roberto, Acosta-Gallegos, Jorge, de la Vega, Octavio Martínez, Simpson, June, 2001. Variability of Mexican isolates of *Macrophomina phaseolina* based on pathogenesis and AFLP genotype. Physiol. Mol. Plant Pathol. 59 (5), 257–264. https://doi.org/10.1006/pmpp.2001.0361.

Mohammed, Afrah, Al-Qahtani, Alaa, al-Mutairi, Amal, Al-Shamri, Bashayir, Aabed, Kawther, 2018. Antibacterial and cytotoxic potential of biosynthesized silver nanoparticles by some plant extracts. Nanomaterials 8 (6), 382. https://doi.org/10.3390/nano8060382.

Mousavi, S., Bagheri, G., Saeidi, S., 2015. Antibacterial Activities of the Hydroalcoholic Extract of *Portulaca oleracea* Leaves and Seeds in Sistan Region. Southeastern Iran. Int. J. Infect. 2, e23214. https://doi.org/10.17795/iji-23214.

Nagarani, G., Abirami, A., Nikitha, P., Siddhuraju, P., 2014. Effect of hydrothermal processing on total polyphenolics and antioxidant potential of underutilized leafy vegetables, *Boerhaavia diffusa* and *Portulaca oleracea*. Asia. Pac. J. Trop. Biomed. 4, S468–S477. https://doi.org/10.12980/apjtb.4.2014c1108.

Nhien, L., Luong, N., Tien, L., Luan, L., 2018. Radiation Synthesis of Silver Nanoparticles/Chitosan for Controlling Leaf Fall Disease on Rubber Trees Causing by *Corynespora cassiicola*. J. Nanomater. 2018, 1–9. https://doi.org/10.1155/2018/7121549.

Oh, K., Chang, I., Hwang, K., Mar, W., 2000. Detection of antifungal activity in *Portulaca oleracea* by a single-cell bioassay system. Phytother. Res. 14, 329–332. https://doi.org/10.1002/1099-1573(200008)14:5<329::aid-ptr581>3.0.co;2-5.

Phu, Dang Van, Lang, Vo Thi Kim, Kim Lan, Nguyen Thi, Duy, Nguyen Ngoc, Chau, Nguyen Duc, Du, Bui Duy, Cam, Bui Duy, Hien, Nguyen Quoc, 2010. Synthesis and antimicrobial effects of colloidal silver nanoparticles in chitosan by γ-irradiation. J. Exp. Nanosci. 5 (2), 169–179. https://doi.org/10.1080/17458080903383324.

Phu, D., Quoc, L., Duy, N., Lan, N., Du, B., Luan, L., Hien, N., 2014. Study on antibacterial activity of silver nanoparticles synthesized by gamma irradiation method using different stabilizers. Nanoscale Res. Lett. 9, 162. https://doi.org/10.1186/1556-276x-9-162.

Qing, Y., Cheng, L., Li, R., Liu, G., Zhang, Y., Tang, X., Wang, J., Liu, H., Qin, Y., 2018. Potential antibacterial mechanism of silver nanoparticles and the optimization of orthopedic implants by advanced modification technologies. Int. J. Nanomedicine 13, 3311–3327. https://doi.org/10.2147/ijn.s165125.

Qostal, S., Kribel, S., Chliyeh, M., Selmaoui, K., Touhami, A.O., Serghat, S., Douira, A., 2019. *Curvularia Spicifera*, A parasite of the fungal complex of root rot of wheat and barley in Morocco. Plant Cell Biotechnol. Mol. Biol. 20, 354–365.

Rahimi, Vafa Baradaran, Ajam, Farideh, Rakhshandeh, Hasan, Askari, Vahid Reza, 2019. A Pharmacological Review on *Portulaca oleracea* L.: Focusing on Anti-Inflammatory, Anti- Oxidant, Immuno-Modulatory and Antitumor Activities. J. Pharmacopunct. 22 (1), 7–15. https://doi.org/10.3831/KPI.2019.22.001.

Seku, Kondaiah, Gangapuram, Bhagavanth Reddy, Pejjai, Babu, Kadimpati, Kishore Kumar, Golla, Narasimha, 2018. Microwave-assisted synthesis of silver nanoparticles and their application in catalytic, antibacterial and antioxidant activities. J. Nanostructure Chem. 8 (2), 179–188. https://doi.org/10.1007/s40097-018-0264-7.

Sharma, G., Nam, J., Sharma, A., Lee, S., 2018. Antimicrobial potential of silver nanoparticles synthesized using medicinal herb *Coptidis* rhizome. Molecules 23, 2268. https://doi.org/10.3390/molecules23092268.

Singh, Chandrashekhar, Kumar, Jitendra, Kumar, Pradeep, Chauhan, Brijesh Singh, Tiwari, Kavindra Nath, Mishra, Sunil Kumar, Srikrishna, S., Saini, Rajesh, Nath, Gopal, Singh, Jasmeet, 2019. Green synthesis of silver nanoparticles using aqueous leaf extract of *Premna integrifolia* (L.) rich in polyphenols and evaluation of their antioxidant, antibacterial and cytotoxic activity. Biotechnol. Biotechnol. Equip. 33 (1), 359–371. https://doi.org/10.1080/13102818.2019.1577699.

Soliman, S., Semreen, M.H., El-Keblawy, A.A., Abdullah, A., Uppuluri, P., Ibrahim, A.S., 2017. Assessment of herbal drugs for promising anti-*Candida* activity. BMC Compl. Alternative Med. 17, 257. https://doi.org/10.1186/s12906-017-1760-x.

Sun, S., Dai, W., Yu, H., Wang, Y., Wang, X., Peng, S., 2015. Antibacterial activity of aqueous and ethanolic extracts of Portulaca oleracea L. and Taraxacum mongolicum Hand. -Mazz against pathogenic bacteria of cow mastitis. Indian J. Anim. Res. 49, 827–829. https://doi.org/10.18805/ijar.5960.

Wang, Yinghui, Wei, Simin, Wang, Kang, Wang, Zhe, Duan, Jinwei, Cui, Lin, Zheng, Huayu, Wang, Ying, Wang, Shanshan, 2020. Evaluation of biosynthesis parameters, stability and biological activities of silver nanoparticles synthesized by *Cornus officinalis* extract under 365 nm UV radiation. RSC Adv. 10 (45), 27173–27182.

Zhang, Li, Wu, Lingli, Si, Youbin, Shu, Kunhui, Mishra, Yogendra Kumar, 2018. Size-dependent cytotoxicity of silver nanoparticles to *Azotobacter vinelandii*: Growth inhibition, cell injury, oxidative stress and internalization. PLoS ONE 13 (12), e0209020. https://doi.org/10.1371/journal.pone.0209020.

Zhou, Yan-Xi, Xin, Hai-Liang, Rahman, Khalid, Wang, Su-Juan, Peng, Cheng, Zhang, Hong, 2015. *Portulaca oleracea* L.: A Review of Phytochemistry and Pharmacological Effects. Biomed Res. Int. 2015, 1–11.